

# Comparative expression analysis of *cysteine-rich intestinal protein* family members *crip1*, *2* and *3* during *Xenopus laevis* embryogenesis

ANNEMARIE HEMPEL<sup>1,2</sup> and SUSANNE J. KÜHL<sup>\*,1</sup>

<sup>1</sup>Institute for Biochemistry and Molecular Biology and

<sup>2</sup>International Graduate School in Molecular Medicine Ulm, Ulm University, Ulm, Germany

**ABSTRACT** Members of the cysteine-rich intestinal protein (Crip) family belong to the group 2 LIM proteins. Crip proteins are widely expressed in adult mammals but their expression profile and function during embryonic development are still mostly unknown. In this study, we have described for the first time the spatio-temporal expression pattern of the three family members *crip1*, *crip2* and *crip3* during *Xenopus laevis* embryogenesis by RT-PCR and whole mount *in situ* hybridization approaches. We observed that all three genes are expressed in the pronephros, branchial arches and the eye. Furthermore, *crip1* transcripts could be visualized in the developing cranial ganglia and neural tube. In contrast, *crip2* could be detected in the cardiovascular system, the brain and the neural tube while *crip3* was expressed in the cranial ganglions and the heart. Based on these findings, we suggest that each *crip* family member may play an important role during embryonic development.

**KEY WORDS:** *Xenopus laevis*, *cystein-rich protein*, *crip1-3*, *LIM*

The first cysteine-rich intestinal protein (CRIP) was discovered as a marker for the suckling-to-weaning transition in the rodent intestine by Birkenmeier and Gordon (Birkenmeier and Gordon, 1986). Among the original names for the different Crip proteins was CRP2 (now Crip2) (Okano *et al.*, 1993), which could easily be mistaken for a cysteine and glycine-rich protein (now classified as CSRP). Both subgroups, Crip and CSRP, belong to the group 2 LIM proteins and consist of three distinct representatives (Birkenmeier and Gordon, 1986, Hempe and Cousins, 1991, van Ham *et al.*, 2003). While Crip1 contains only one single LIM domain, Crip2 and Crip3 carry two of them (Kirchner *et al.*, 2001, Nalik *et al.*, 1989, Wang *et al.*, 1992). Such differences could be the result of DNA duplication events (Nalik *et al.*, 1989). The LIM domain is a conserved cysteine-histidine-rich sequence with a double zinc-finger with the consensus sequence (CX<sub>2</sub>CX<sub>17</sub>HX<sub>2</sub>C)-X<sub>2</sub>-(CX<sub>2</sub>CX<sub>17</sub>CX<sub>3</sub>C) (Bach, 2000, Liebhaber *et al.*, 1990). LIM domains are postulated to promote protein-protein interactions exemplified by the interaction between the LIM domain of Crip2 and the PDZ domain IV of PTP-BL (protein tyrosine phosphatase PTP-BL five) (Bach, 2000, van Ham *et al.*, 2003). Furthermore, the LIM domain is known to bind zinc that probably accounts for the zinc-binding properties of

Crip1 reported by Hempe and Cousins (Hempe and Cousins, 1991, Hempe and Cousins, 1992). In addition, the zinc-dependent metalloprotease ADAM19 facilitate Crip2 secretion (Tanabe *et al.*, 2010).

In adult mammals, all *crip* genes exhibit a wide tissue distribution, which might indicate essential roles in diverse cellular functions (Birkenmeier and Gordon, 1986, Casrouge *et al.*, 2004, Chung *et al.*, 2011, Hallquist *et al.*, 1996, Karim *et al.*, 1996, Kirchner *et al.*, 2001, Levenson *et al.*, 1993, Nalik *et al.*, 1989, Okano *et al.*, 1993, Tsui *et al.*, 1994, van Ham *et al.*, 2003, Wang *et al.*, 1992, Yu *et al.*, 2002). The different *crip* members have been linked to tissue differentiation and remodeling, immune response as well as suppression of angiogenesis and tumorigenesis (Chung *et al.*, 2011, Davis *et al.*, 1998, Hallquist *et al.*, 1996, Khoo *et al.*, 1996, Lanningham-Foster *et al.*, 2002, Wei *et al.*, 2011).

However, little is known about the expression profiles or functions of the *crip* family members during early embryogenesis in

---

*Abbreviations used in this paper:* crip, cysteine-rich intestinal protein; LIM, Lin11, Isl-1 and Mec-3; RT-PCR, reverse transcription polymerase chain reaction; WMISH, whole-mount *in situ* hybridization; X. laevis/tropicalis, *Xenopus laevis/tropicalis*.

---

\*Address correspondence to: Susanne J. Kühl, Institute for Biochemistry and Molecular Biology, Ulm University, Albert-Einstein-Allee 11, 89081 Ulm, Germany. Tel: ++49-731-500-23283. Fax: ++49-731-500-23277. E-Mail: susanne.kuehl@uni-ulm.de

Supplementary Material (four figures) for this paper is available at: <http://dx.doi.org/10.1387/ijdb.140270sk>

Accepted: 19 December 2014.

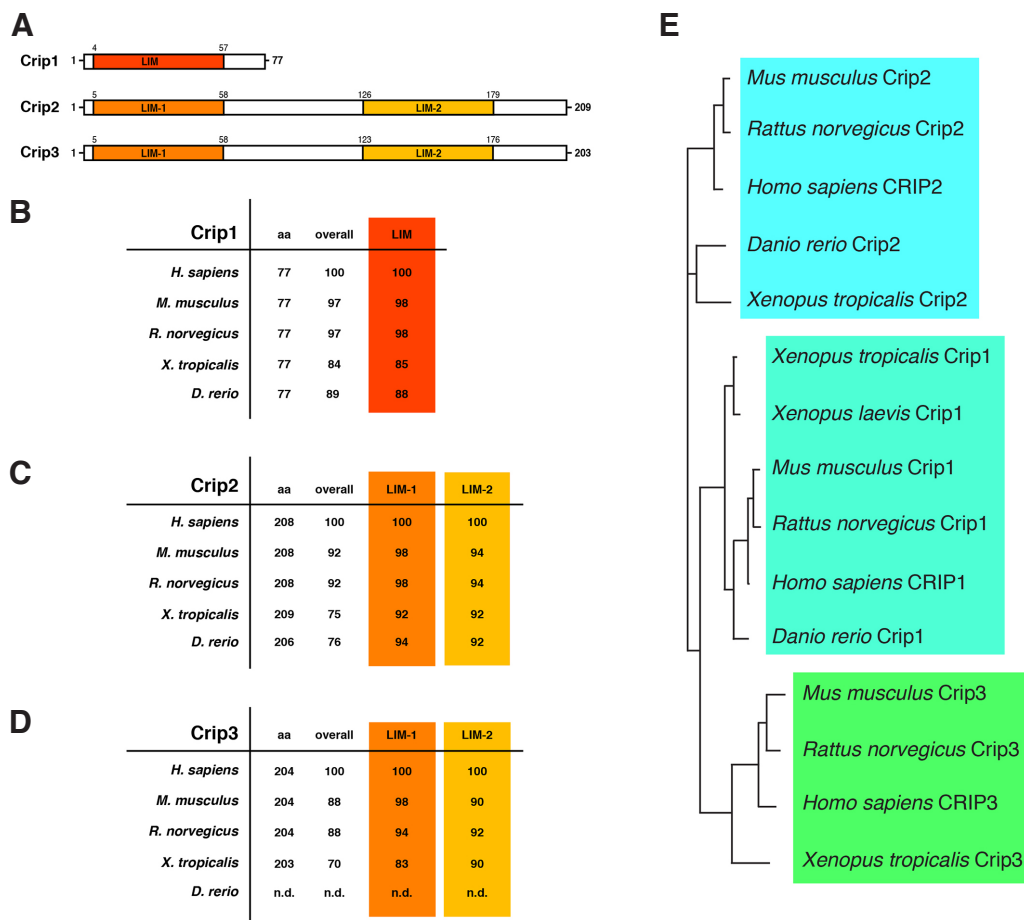


**Fig. 1. Crip1, Crip2 and Crip3 in *Xenopus*.** (A) Schematic representation of *X. tropicalis* Crip1, Crip2 and Crip3 protein domains. Crip1 contains one LIM domain, while Crip2 and Crip3 have two (LIM-1 and -2) each. (B-D) Homology of the amino acid sequences of the full length (overall) and individual LIM domains of the Crip proteins among different species. Numbers represent similarities of the indicated species in percentage compared to *Homo sapiens*. (E) Phylogenetic tree for the Crip sequences whose primary amino acid sequence alignment is shown in (A). aa, amino acid length in numbers; CRIP, cysteine-rich intestinal protein; LIM, Lin11, Isl-1 and Mec-3.

any organism. In this study, we present the specific expression pattern of *crip1*, *crip2* and *crip3* throughout early *Xenopus laevis* embryogenesis, which are fundamental information for future functional analyses. We thus provide in this paper the first comparative embryonic expression analyses of all three *crip* genes in a vertebrate organism.

## Results and Discussion

### *Xenopus* cysteine-rich protein family members

So far no expression or functional data have been reported about the different members of the cysteine-rich protein family in *Xenopus*. For an initial analysis of *crip* genes in *Xenopus*, we relied on publicly available *Xenopus laevis/tropicalis* sequences. The predicted protein sequences of each Crip family member were highly conserved across species (Fig. 1 B-D). While Crip1 contained only one LIM-domain, both Crip2 and Crip3 contained two LIM domains (LIM-1 and -2) (Fig. 1A), all of which were highly conserved among different species (Fig. 1 B-D). Nevertheless, all three Crip family members are closely related as phylogenetic analysis showed (Fig. 1E). Furthermore, synteny analyses showed

that *crip1* and *crip2* are neighbouring genes. Their gene loci and their neighbouring genes are highly conserved between *Homo sapiens*, *Mus musculus*, *Rattus norvegicus* and *Xenopus tropicalis* (Fig. 2A). Surprisingly, in the *Xenopus tropicalis* genome, the genes *pacs2*, *mta1* and *crip1* had been inverted compared to the genomes of human, mouse and rat for unknown reasons. The gene loci of *crip3* and its neighbouring genes are highly conserved between *Homo sapiens*, *Mus musculus* and *Rattus norvegicus* as well (Fig. 2B). The available *Xenopus tropicalis* genomic region covering *crip3* (Gene ID 548528) is too short for a detailed analysis and can therefore not be compared with the gene loci of other organisms. The preserved protein structures and gene localizations of the individual Crip family members suggest a conserved expression as well as conserved function of the *crip* genes across species.

To investigate the temporal expression pattern of *crip1-3* during *Xenopus laevis* embryogenesis, semi-quantitative reverse transcription polymerase chain reaction (RT-PCR) experiments using *Xenopus laevis* specific *crip1-3* primer pairs (Suppl. Figs. 1-3) were performed. Whereas *crip1* and *crip2* transcripts were first detected during gastrulation as early as stage 10 and 12.5

respectively, *crip3* was maternally supplied and continuously expressed throughout early embryogenesis (Fig. 3).

We next analyzed the spatio-temporal expression of all three *crip* family members during *Xenopus laevis* embryogenesis by whole-mount *in situ* hybridization (WMISH). For further tissue-specific analysis, vibratome sections using stained embryos were performed. To examine the expression profiles of all three *crip* family members, we cloned *Xenopus laevis* specific cDNA fragments with the length of 550 bp (*crip1*), 539 bp (*crip2*) and 492 bp (*crip3*) and generated *antisense* DIG-labelled RNA probes (Suppl. Figs. 1-3). To show the specificity of these probes, we performed a dot blot indicating the usability of the signed probes (Suppl. Figure 4).

**Expression of *crip1* during *Xenopus* embryogenesis**

The first tissue-specific expression of *crip1* was detected during gastrulation (data not shown) and became manifested at stage 13 in the anterior neural plate (Fig. 4B) being in line with the RT-PCR data. At stage 20, *crip1* was expressed in the developing neural tissue (Fig. 4C). At stage 25, *crip1* transcripts were detected at the dorsal side of the embryo and in the migrating cranial neural crest cells (Fig. 4D). In early tailbud stages, *crip1* was strongly expressed in the neural crest derived part of the second and third branchial arches and at the dorsal aorta and in the blood islands as well (Fig. 4 E-F, I; Fig. 5 G-J, T). Furthermore, *crip1* was clearly visible in the neural roof plate and the ventral region of the neural tube at stage 33 (Fig. 5K) and at the neural floor plate at stage 38

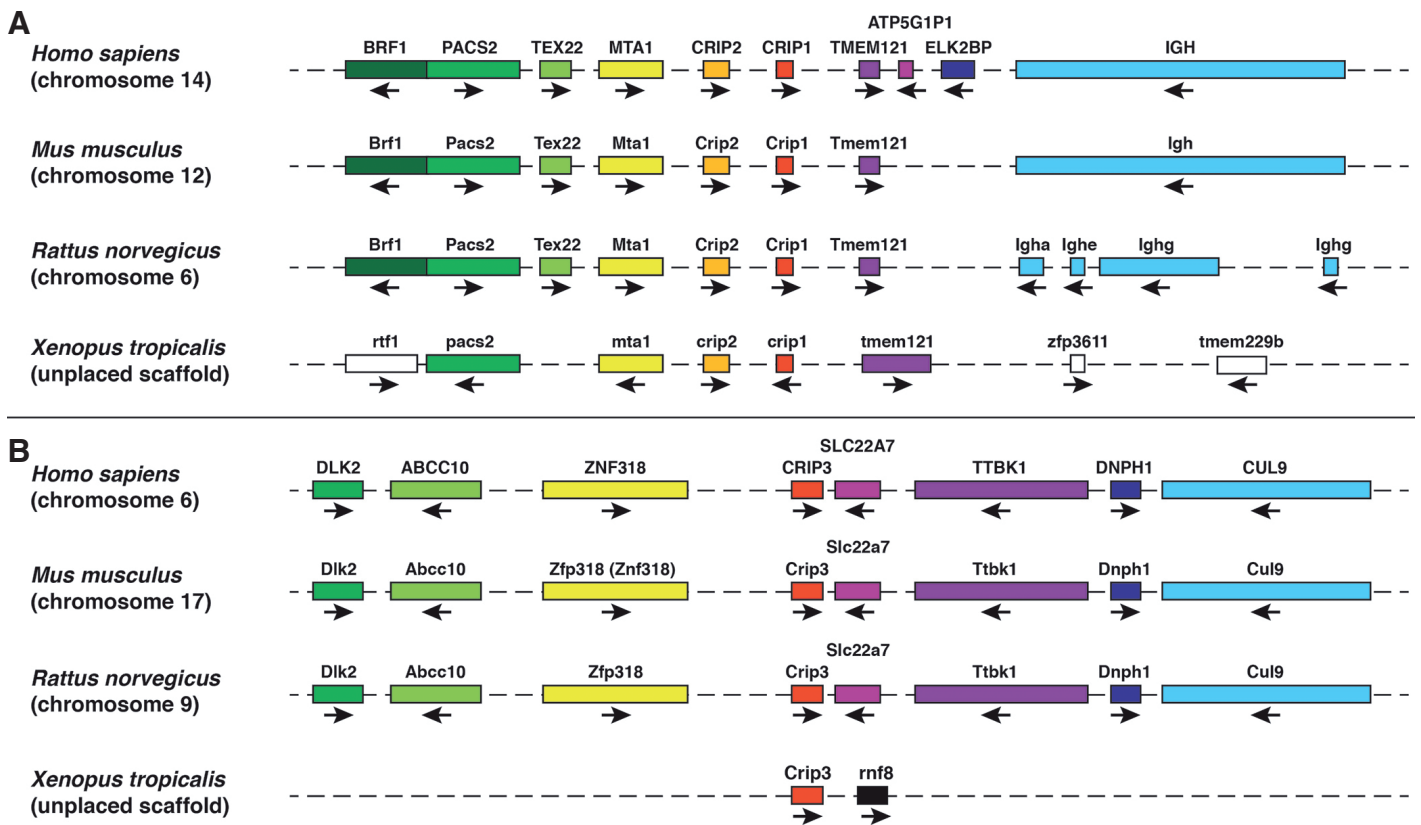


**Fig. 2. Synteny analyses of the *crip* family members in *Homo sapiens*, *Mus musculus*, *Rattus norvegicus*, *Xenopus tropicalis* and *Danio rerio*.** (A) The schematic overview shows the comparison of the *crip1* and *crip2* genes and their neighbouring gene loci in *H. sapiens* (chromosome 14), *M. musculus* (chromosome 12), *R. norvegicus* (chromosome 6) and *X. tropicalis* (unplaced scaffold). (B) The schematic overview shows the comparison of the *crip3* gene and its neighbouring gene loci in *H. sapiens* (chromosome 6), *M. musculus* (chromosome 17), *R. norvegicus* (chromosome 9) and *X. tropicalis* (unplaced scaffold). The gene length and distances between them are not drawn to scale. Conserved genes are indicated by the same color code and non-conserved genes by white boxes. The orientation of the genes open reading frames are depicted by black arrows. Abcc10 ATP-binding cassette sub-family C (CFTR/MRP) member 10, asxl2 additional sex combs like 2 (Drosophila), ATP5G1P1 ATP synthase, H+ transporting, mitochondrial Fo complex, subunit C1 (subunit 9) pseudogene 1, BRF1 BRF1 RNA polymerase III transcription initiation factor 90 kDa subunit, CUL9 cullin 9, DLK2 delta-like 2 homolog (Drosophila), DNPH1 2'-deoxynucleoside 5'-phosphate N-hydrolase 1, dtnbb dystrobrevin beta b, ELK2BP ELK2B member of ETS oncogene family pseudogene, hadhab hydroxyacyl-CoA dehydrogenase/3-ketoacyl-CoA thiolase/enoyl-CoA hydratase (trifunctional protein) alpha subunit b, IGH immunoglobulin heavy locus/immunoglobulin heavy chain complex, Igha immunoglobulin heavy chain alpha, Ighe immunoglobulin heavy chain (epsilon polypeptide), Ighg immunoglobulin heavy chain (gamma polypeptide), kif3cb kinesin family member 3Cb, mta1 metastasis associated 1, pacs2 phosphofurin acidic cluster sorting protein 2, ptgr2 prostaglandin reductase 2, rnf8 ring finger protein 8, E3 ubiquitin protein ligase, rtf1 Rtf1 Paf1/RNA polymerase II complex component homolog, SLC22A7 solute carrier family 22 (organic anion transporter) member 7, slc25a21 solute carrier family 25 (mitochondrial oxodicarboxylate carrier) member 21, slc30a1b solute carrier family 30 (zinc transporter) member 1b, TEX22 testis expressed 22, tmem121 transmembrane protein 121, tmem229b transmembrane protein 229b, tmem62 transmembrane protein 62, TTBK1 tau tubulin kinase 1, zfp3611a zinc finger protein 36 C3H type-like 1a, ZNF318/Zfp318 zinc finger protein 318.

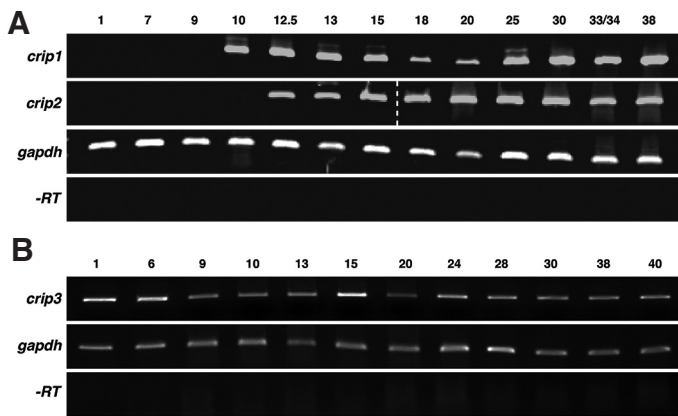


**Fig. 3.** Temporal expression patterns of *crip1-3* during *Xenopus laevis* embryogenesis analysed by semi-quantitative RT-PCR approaches with cDNA templates of the indicated stages. As loading control *gapdh* (glyceraldehyde-3-phosphate dehydrogenase) and as negative controls *-RT* (reverse transcriptase) reactions lacking the enzyme reverse transcriptase were used. **(A)** *Crip1* and *crip2* expression were first detected during gastrulation at stage 10 and 12.5 respectively and continuously expressed till stage 38. **(B)** In contrast *crip3* transcripts were maternally supplied and continuously expressed till stage 40.

(Fig. 5T). At stage 38 and 41, *crip1* was expressed in the anlagen of the developing cartilage structures including the quadrate cartilage, Meckel's cartilage, ceratobranchial cartilage and ceratohyal cartilage as well as the branchial arches (Fig. 4 G-H; Fig. 5 M-O). Additionally, *crip1* was found in the sensory layer of the epidermis and the ganglion cell layer of the retina (Fig. 5 N,S). Moreover, a specific *crip1* expression could be detected in the cardiac arteries, the second heart field and the ventral aorta (Fig. 4 J-K; Fig. 5 M,P-R). These results are in line with data by others demonstrating *CRIP1* mRNA expression in fetal rat and human hearts (Tsui *et al.*, 1994). *Crip1* transcripts were also detected in the tubules of the developing pronephros (Fig. 5U) and lung (Fig. 5V). Not much is known about *crip1* expression during early embryogenesis in other vertebrate species. Further studies will be required to determine whether *crip1* expression is conserved across species.

#### Expression of *crip2* during *Xenopus* embryogenesis

The tissue-specific expression of *crip2* started during gastrulation (data not shown) what is in agreement with RT-PCR results. At stage 13, *crip2* was strongly expressed in the anterior neural plate (Fig. 6A). At stage 23, *crip2* was expressed in the anterior neural tissue (Fig. 6B) and at stage 25 at the dorsal side of the embryo and the migrating neural crest cells (Fig. 6C). In tailbud stages,

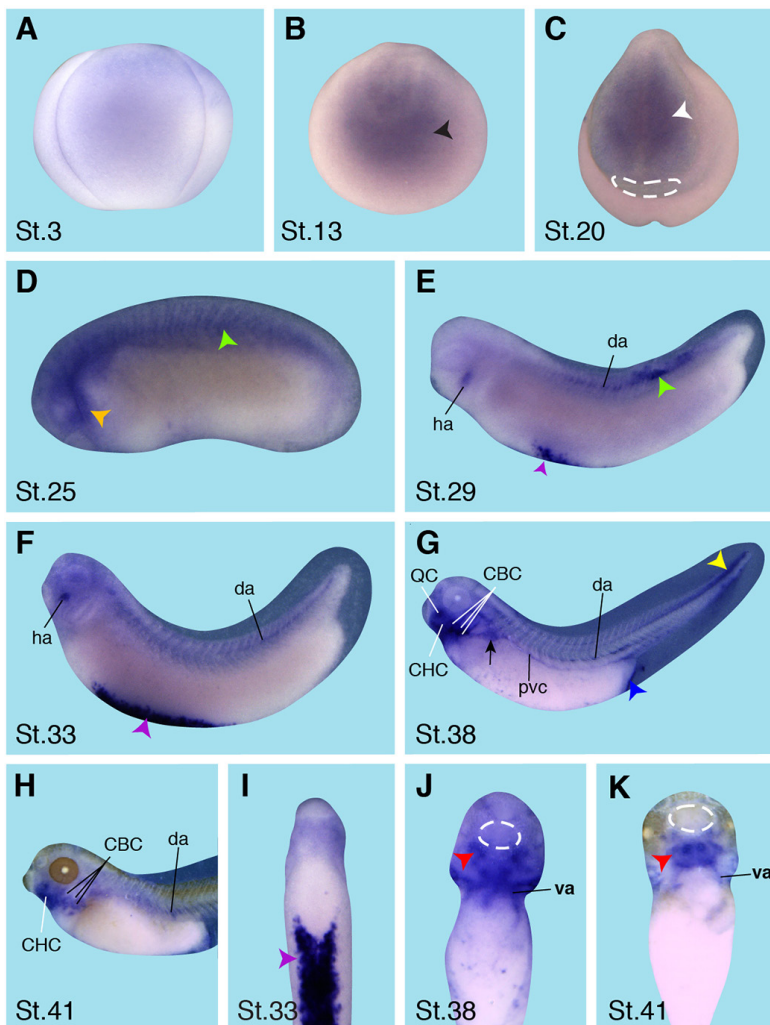


**Fig. 4.** *Crip1* spatial expression pattern during *X. laevis* embryogenesis. Embryonic stages are indicated in each panel. The white dashed circles depict the cement gland. **(A)** At stage 3, embryos were negative for *crip1* expression (lateral view). **(B)** Anterior view of a stage 13 embryo. *Crip1* was expressed in the anterior neural plate (black arrowhead). **(C)** The anterior view of a stage 20 embryo shows *crip1* expression in the anterior neural tissue (white arrowhead). **(D-H)** Lateral views with anterior to the left. **(I-K)** Ventral views with anterior to the top. **(D)** At stage 25 *crip1* transcripts were detected in the migrating cranial neural crest cells (orange arrowhead) and at the dorsal side of the embryo (green arrowhead). **(E-F, I)** *Crip1* was expressed in the hyoid arch (ha), in the dorsal aorta (da) with a stronger expression in the posterior part (green arrowhead) and in the ventral blood islands (violet arrowhead). **(G-H)** In later stages *crip1* transcripts were strongly detected in the head mesenchyme, namely the quadrate cartilage (QC), ceratobranchial cartilage (CBC), and ceratohyal cartilage (CHC) as well as. *Crip1* transcripts were in the dorsal aorta (da) detected. Furthermore, *crip1* was expressed in the pronephric tubule convolute (black arrow) and in the posterior cardinal vein (pcv). The stomadeum including the region where the cloaca will form (blue arrowhead) as well as the tip of the tail (yellow arrowhead) showed a strong *crip1* expression, too. **(J-K)** Also the second heart field (red arrowhead) and ventral aorta (va) were positive for *crip1*.

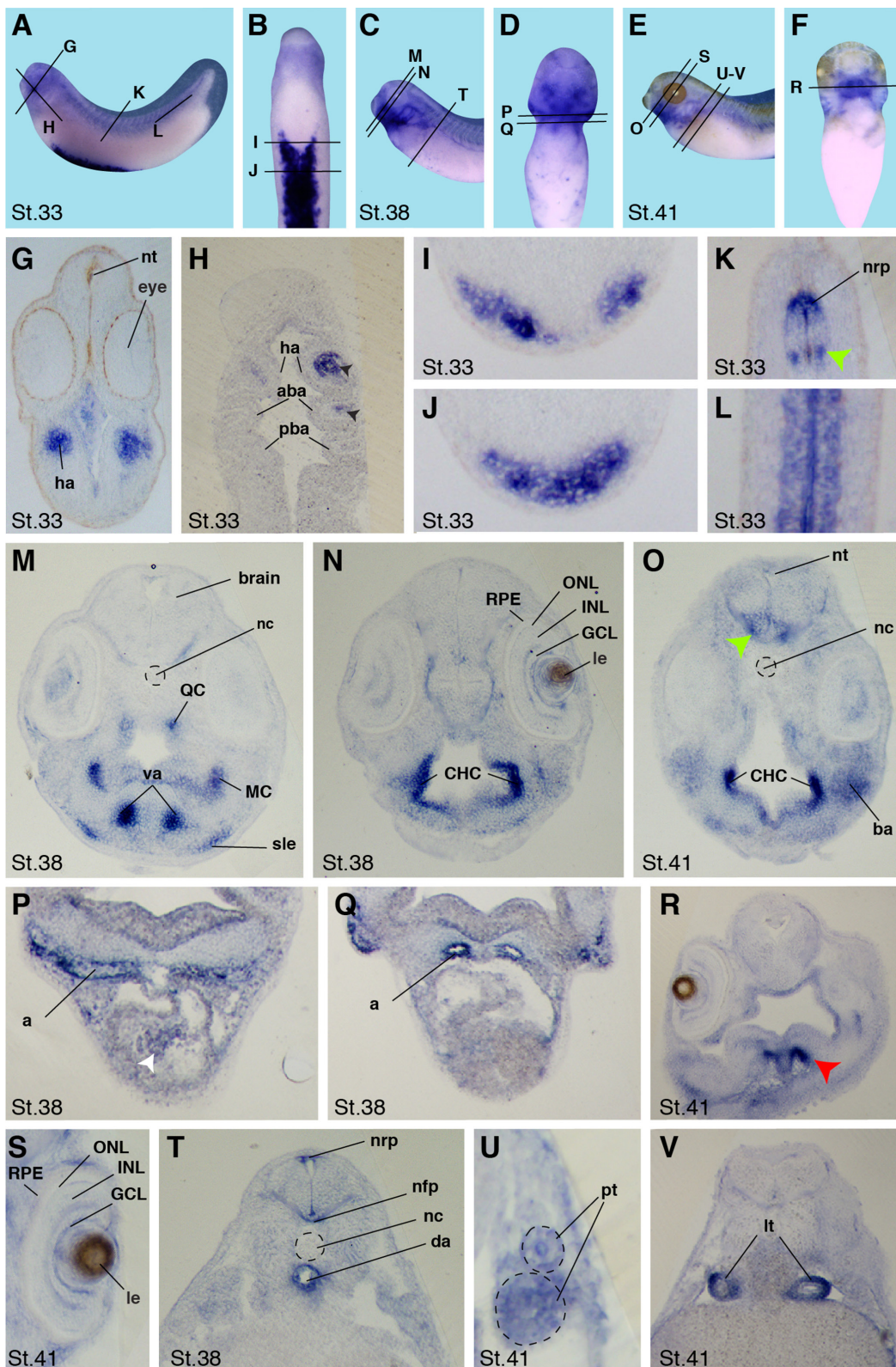


**Fig. 5. Tissue specific expression of *crip1* in *Xenopus* embryos stage 33, 38 and 41. (A,C,E) Lateral views with anterior to the left. (B,D,E) Ventral views with anterior to the top. Black lines indicate level of sections shown in G-V. (G,I-K,M-V) Transversal sections with the dorsal side to the top. (H, L) Horizontal sections with anterior to the top. The notochord (nc) and pronephric tubules (pt) are depicted by dashed circles, respectively (M,O,T,U). (G-H) At stage 33 *crip1* transcripts were detected in the neural crest derived part of the second and third branchial arches namely the hyoid arch (ha) and the anterior branchial arch (aba) but not in the posterior third branchial arch (pba) (black arrowheads). (I-L) Furthermore, *crip1* was strongly expressed in the blood islands (I-J) and neural roof plate (nrp) and a specific ventral region of the neural tube (green arrowhead) (K-L). (M-O) Later, *crip1* was strongly expressed in the ventral aorta (va), in the sensory layer of the epidermis (sle) and the cranial cartilage structures as indicated: quadrate cartilages (QC), Meckel's cartilages (MC), ceratohyal cartilages (CHC) as well as in the branchial arches (ba).**

(N,S) Additionally *crip1* was found in the ganglion cell layer (GCL) of the eye. (O,T) Similar to stage 33, at stage 38 *crip1* was expressed ventral part of the neural tube (green arrowhead), the neural roof plate (nrp) and in the neural floor plate (nfp). (T) Furthermore, *crip1* transcripts were detected in the surrounding layer of the dorsal aorta (da). (P-R) Sections through the heart region revealed *crip1* expression in the arteries (a), at stage 38 weakly in the endocardium (white arrowhead) and at stage 41 in the second heart field (red arrowheads). (U-V) At stage 41 *crip1* was expressed in the pronephric tubules (pt) and in the lung tubes (lt). le, lens; INL and ONL, inner and outer nuclear layer; RPE, retinal pigmented epithelium.

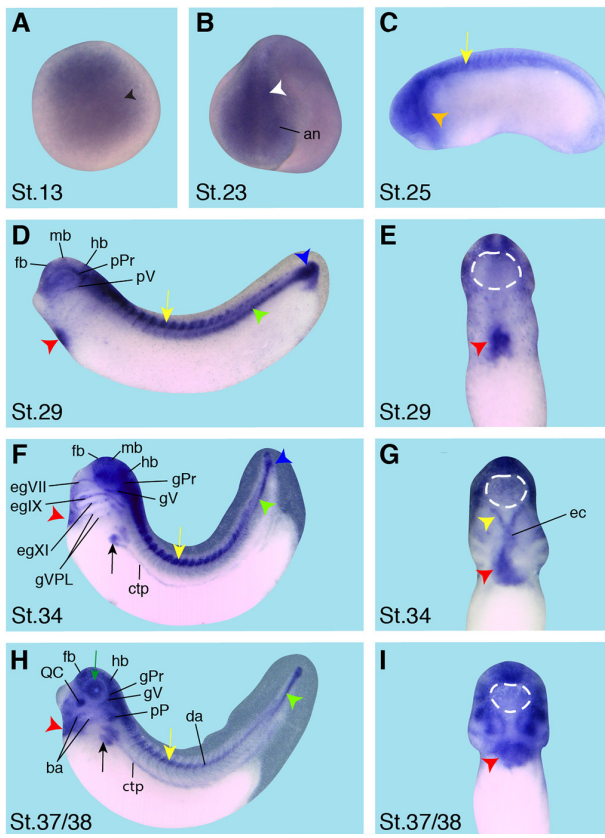
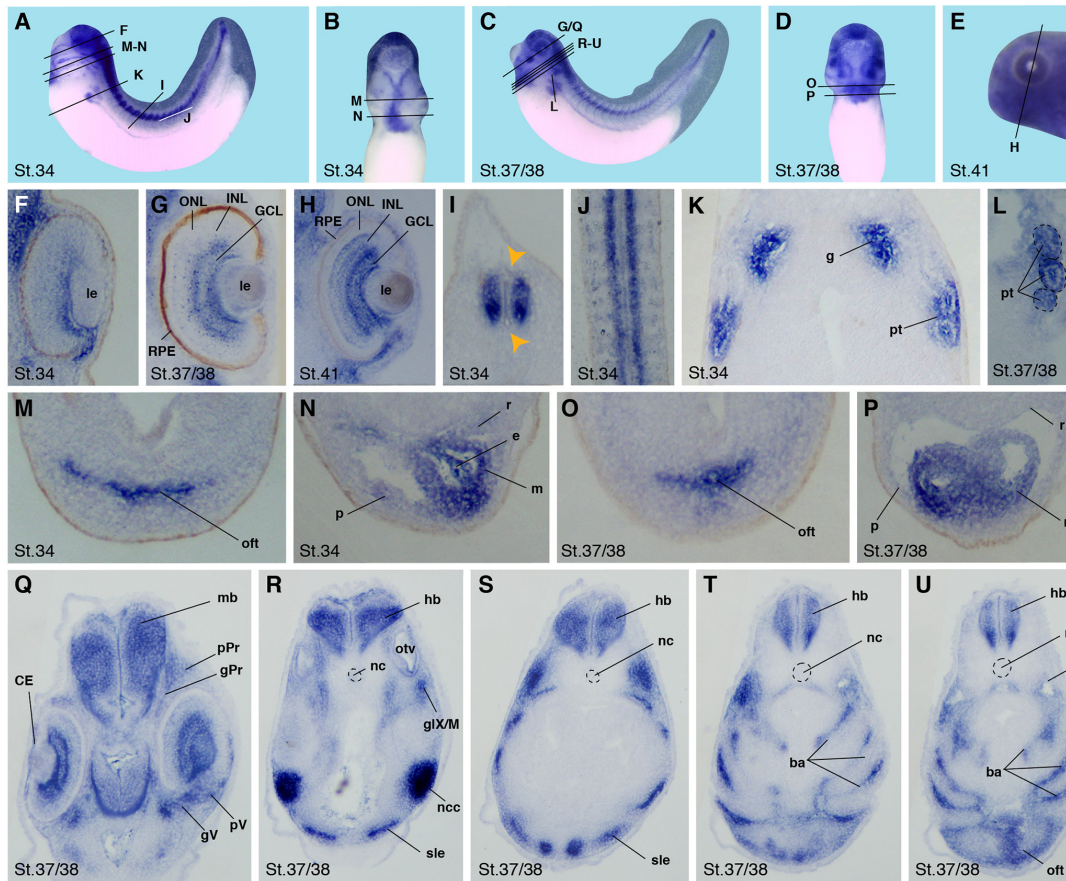


**Fig. 6 (Left). Spatial expression pattern of *crip2* during *X. laevis* embryonic development.** Embryonic stages are indicated in each panel. The cement gland is depicted as white dashed circles. **(A)** Animal view of a stage 13 embryo. *crip2* expression was detected in the anterior neural plate (black arrowhead). **(B)** The anterior view of a stage 23 embryo showed a *crip2* expression in the anterior neural tissue (an) and the neural tube (white arrowhead). **(C-D,F,H)** Lateral views with anterior to the left. **(E,G,I)** Ventral views with anterior to the top. **(C)** At stage 25 *crip2* transcripts were detected in the migrating cranial neural crest cells (orange arrowhead) and the dorsal side of the embryo (yellow arrow). **(D-I)** *Crip2* was expressed in the cardiac tissue especially of the first heart field (red arrowheads), the endocardium (ec) and the cardiac vascular nerves (yellow arrowhead). **(D)** At stage 29 *crip2* transcripts were strongly detected at the dorsal side (yellow arrow), the posterior cardinal vein (green arrowhead) and at the tip of the tail (blue arrowhead). Furthermore, *crip2* was expressed in the fore-, mid- and hindbrain (fb, mb, hb) as well as in the profundal placode (pPr) and the trigeminal placode (pV). **(F,H)** Later during organogenesis *crip2* transcripts were additionally detected in the anterior part of pronephros (black arrow) and the connecting tubule of the pronephros (ctp). **(F)** At stage 34 the profundal ganglion (gPr), the trigeminal ganglion (gV), the facial epibranchial ganglia egVII, egIX and egXI and the cells that contribute to the vagal and posterior lateral line ganglion (gVPL) were positive for *crip2*. **(H)** At stage 37/38 *crip2* was also expressed the quadrate cartilages (QC), branchial arches (ba) and dorsal aorta (da).

**Fig. 7 (Bottom). *Crip2* tissue specific expression in *Xenopus* embryos stage 34, 37/38 and 41.** **(A,C,E)** Lateral views with anterior to the left. **(B,D)** Ventral views with anterior to the top. Black lines show level of sections demonstrated in F-U. **(F-I,K,M-U)** Transversal sections with the dorsal side to the top. **(J, L)** Horizontal sections with anterior to the top. The notochord (nc) and pronephric tubules (pt) are depicted by dashed circles, respectively **(L,R-U)**. **(F-H)** During *Xenopus* embryogenesis *crip2*



was expressed in the developing eye, more precisely the ganglion cell layer (GCL). In contrast, no expression was detected in the lens (le), the inner and outer nuclear layer (INL, ONL) or the retinal pigmented epithelium (RPE). **(I,J)** At stage 34 *crip2* was found in the neural tube except at the most dorsal and ventral parts (orange arrowheads). **(K,L)** Furthermore, *crip2* expression was detected in the glomerulus (g) and the specific pronephric tubules (pt). **(M-P)** Cardiac sections at stage 34 and 37/38 revealed *crip2* expression in the outflow tract (oft), the pericardial roof (r) as well as the myo- and endocardium (m, e) of the developing heart, but not the pericardium (p). **(Q-U)** *Crip2* was expressed in various tissue of the brain, predominantly in the mid- and hindbrain (mb, hb). The ganglia and placodes of the profundal (gPr, pPr) and trigeminal (gV, pV) show distinct *crip2* expression as well as the cornea epithelium (CE). **(Q)** **(R-I)** Consecutive transversal sections at the level of the otic vesicle (otv) showed *crip2* transcripts in the sensory layer of epidermis (sle), neural crest cells (ncc), the fused ganglia of the glossopharyngeal and middle lateral line nerves (glX/M) and the branchial arches (ba).

*crip2* transcripts were detected in various parts of the brain (Fig. 7 Q-U) as well as in the posterior neural tube (Fig. 7I). Note, that in the neural tube, differentiated neurons were *crip2* positive whereas neural stem cells located in the centre of the neural tube were negative for *crip2*. The facial epibranchial ganglia egVII, egIX and egXI, the cells that contribute to the vagal and posterior lateral line ganglion as well as the placodes and ganglia of the profundal and trigeminus nerve also showed distinct *crip2* expression at sages 34 (Fig. 6 D,F). Additionally, *crip2* was expressed in the sensory layer of the epidermis, neural crest cells, the fused ganglia of the glossopharyngeal and middle lateral line nerves (Fig. 6F; Fig. 7Q-S) and the branchial arches (Fig. 6H; Fig. 7 T-U). In the ganglion cell layer of the eye, *crip2* transcripts were detected as well (Fig. 7 F-H). Furthermore, *crip2* expression was visualized in the developing pronephros (Fig. 6 F,H; Fig. 7 K-L) and in the pericardial roof, the myo- and endocardium of the developing heart (Fig. 6 D-I; Fig. 7 M-P).

The spatio-temporal expression of *Crip2* during embryogenesis was also described in more detail in mice and zebrafish (Sun *et al.*, 2008, Wei *et al.*, 2011, Yu *et al.*, 2002). *Crip2* is detected in pre-streak embryo, up-regulated with the onset of gastrulation and shows an abundant expression throughout the developing heart which is consistent with our expression study. Later during murine embryogenesis, *Crip2* is expressed in the heart primordial (E7.5), heart tube (E8.5) and strongly in the myo- and endocardium as well as the coronary vascular endothelial cells in the atrium and ventricle of embryonic (E9.5-15.5) and adult mouse hearts. Again, this is in agreement with *crip2* expression in *Xenopus*. Additionally, murine *Crip2* was detected in lymphatic endothelial cells, in dorsal root ganglia and around the spinal cord, the neural tube including the brain, lungs, pelvic ganglia and mesenchyme of the lower urinary tract, but not in the kidney (Wei *et al.*, 2011, Wiese *et al.*, 2012, Yu *et al.*, 2002, Zhang *et al.*, 2005). In zebrafish, *crip2* transcript were detected the earliest in the premigratory neural crest cells in rhombomere 6 of the neural tube, in the cardiac progenitor cells in anterior lateral plate mesoderm and mesoendodermal cells in the primary heart field (6- to 20-somite stage). Later during zebrafish embryogenesis, *crip2* was expressed in the heart tube, ventricular cardiomyocytes and aortic vessels in pharyngeal arches 3-6 (24-36 hpf) (Sun *et al.*, 2008). Hence, *crip2* was recently used as cardiac neural crest cell marker (Wang *et al.*, 2013). Collectively, these data indicate a conserved expression of *crip2* across species.

#### Expression of *crip3* during *Xenopus* embryogenesis

Like in the RT-PCR experiments, *crip3* transcripts could be detected early on by WMISH approaches. At stage 3, *crip3* was visualized in the animal half of the embryo (Fig. 8A). At stage 13,

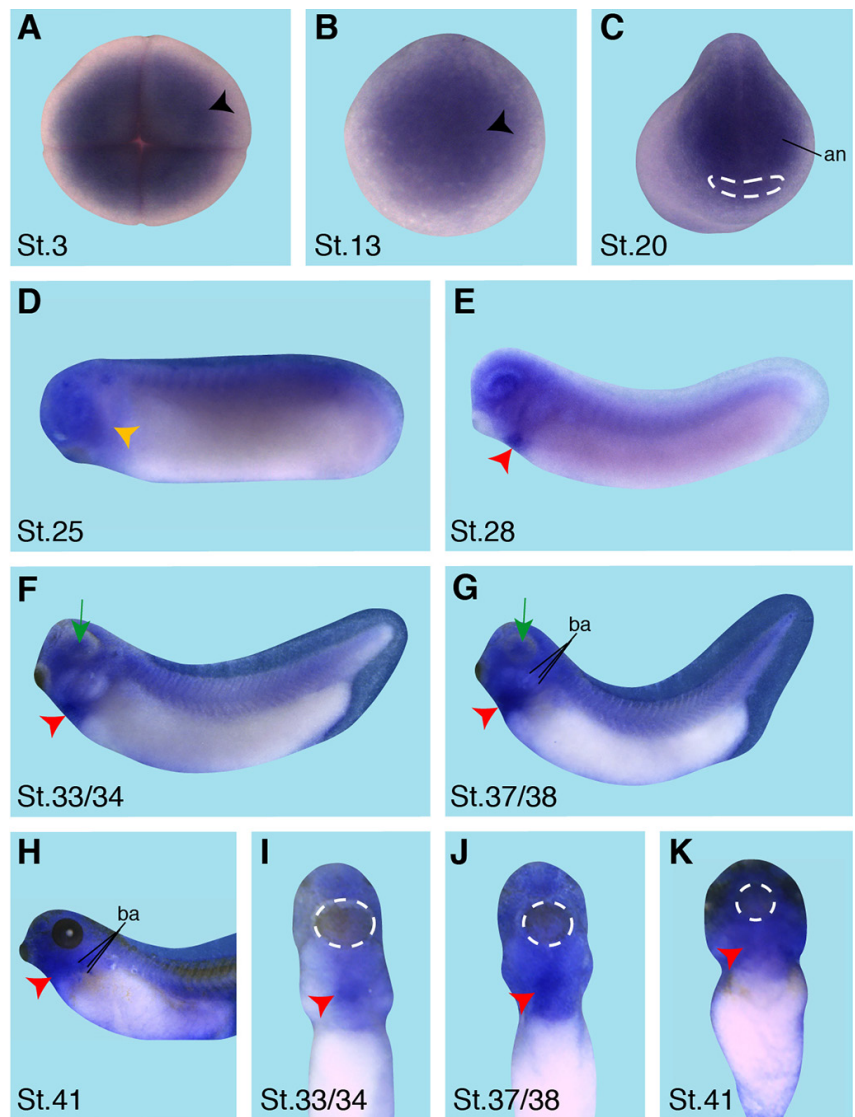


**Fig. 8. Spatial expression of *crip3* during *X. laevis* embryogenesis.** Embryonic stages are indicated in each panel. The white dashed circles depict the cement gland. (A) Animal view. *Crip3* expression was detected at the animal half at 4-cell stage (black arrowhead). (B) *Crip3* is expressed in the anterior neural plate. (C) The anterior view of a stage 20 embryo showed *crip3* expression in the anterior neural tissue (an). (D-H) Lateral views with anterior to the left. (I-K) Ventral views with anterior to the top. (D-H) At stage 25 and 29 *crip3* was expressed in the migrating neural crest cells (orange arrowhead in (D,E)) and at later stages in the branchial arches (ba, G,H). (F,G) During organogenesis a very weak *crip3* signal was seen in the dorsal side of the embryo (green arrowheads). (E-K) Furthermore, during *Xenopus* embryogenesis *crip3* was detected in the developing eye (green arrow) and cardiac tissue (red arrowheads).

*crip3* was expressed in the anterior neural plate (Fig. 8B) and later in the anterior neural tissue (Fig. 8C). During stage 33/34 *crip3* was weakly expressed in a subpopulation of differentiated neurons in the midbrain (Fig. 9B). In later tailbud stages, *crip3* was strongly expressed in the branchial arches (Fig. 9N) as well as in the peri-, myo- and endocardium and the pericardial roof of the developing heart (Fig. 8 E-K; Fig. 9 H-I). A very faint expression was also detected in the developing pronephros and in the anlage of the ceratohyal cartilage (Fig. 9 G,M). Furthermore, *crip3* was located in the cornea epithelium of the developing eye at stage 33/34 and

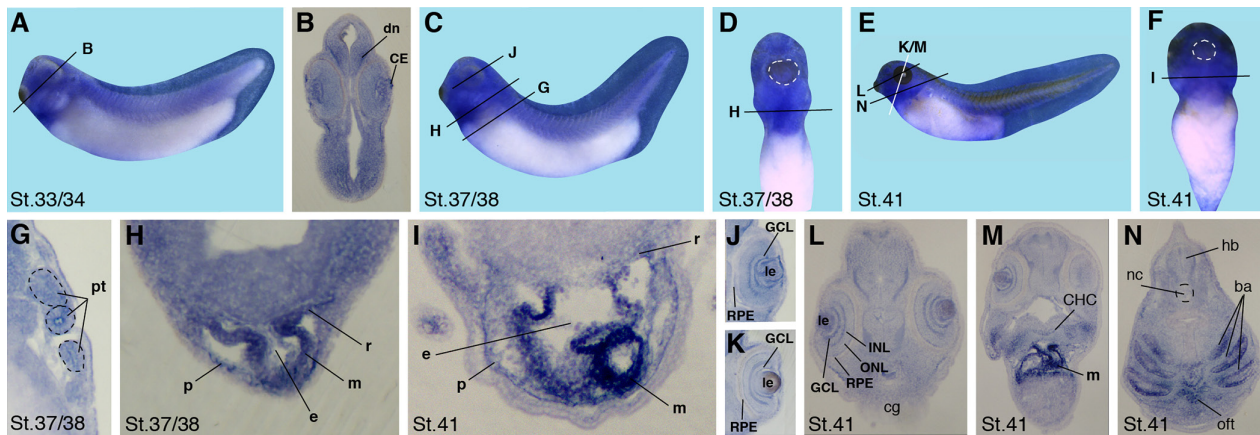


**Fig. 9. Tissue specific expression of *crip3* in *Xenopus* embryos stage 33/34, 38 and 41. (A,C,E) Lateral views with anterior to the left. (D,F) Ventral views with anterior to the top. White dotted circles depict the cement gland. (B, G-N) Transversal vibratome sections through different regions of the embryos with the dorsal to the top as indicated by the lines shown in A,C-F. The pronephric tubules (pt) and notochord (nc) are depicted by dashed circles, respectively (G,N). (B,G) *Crip3* transcripts were weakly expressed in the differentiated neurons (dn, B) and in the pronephric tubules (pt, G). (H-I,M-N) The strongest expression of *crip3* was found in the developing heart, namely the outflow tract (oft), the peri- and myocardium (p, m) as well as in the pericardial roof (r) and endocardium (e). (B,J-L) Sections through the eye showed a weak *crip3* expression in the cornea epithelium (CE) at stage 33/34 (B) and in the ganglion cell layer (GCL) and lens (le) at stage 37/38 and 41, while the inner and outer nuclear layers (INL, ONL) and the retinal pigmented epithelium (RPE) were negative for *crip3* (J-L). (M-N) At stage 41 *crip3* was expressed in the ceratohyal cartilage (CHC) and the branchial arches (ba). cg cement gland, hb hindbrain.**

in the lens and the retina, in particular the ganglion cell layer, at stages 37/38 and 41 (green arrows in Fig. 8 E-H; Fig. 9 B,J,L).

Little is known about the embryonic *crip3* expression in other organisms. Human *CRIP3* could be detected in the fetal thymus, spleen, brain, heart, kidney, liver and lung partially in line with our observations (Casrouge *et al.*, 2004). These limited findings make a comparison of the expression across species difficult.

As all three *crip* family members show a distinct expression pattern during early *Xenopus* development (Table 1), it would be interesting to examine their function during embryonic development by using knock-down approaches in future studies.

## Material and Methods

### *Xenopus laevis* embryos

*Xenopus* embryos were obtained, cultured according to standard protocols (Sive *et al.*, 2000) and staged according to (Nieuwkoop and Faber, 1994).

### Cloning of *Xenopus laevis* *crip1-3*

*X. laevis* cDNA fragments of 550 bp (*crip1*; Acc. No. KP036486), 539 bp (*crip2*; Acc. No. KP036487) and 492 bp (*crip3*; Acc. No. KP036488) were cloned into the pSC-B vector (Stratagene, La Jolla, Ca) by using cDNAs from stages 28 (*crip1*), 33 (*crip3*) or 42 (*crip2*) of *X. laevis* embryos. The primers were designed according to conserved sequence regions (*X. laevis*

*crip1*-a:NM\_001093834.1; *X. tropicalis**crip2*:NM\_001079267.1; *X. tropicalis* *crip3*:NM\_001015811.1). Following cloning primers were used: *crip1*<sub>a</sub>\_forw: 5'-CACCAGCAACATGCCCAAGTGT-3'; *crip1*<sub>a</sub>\_rev: 5'-GTAAACATA-ATATACACCTGCTTGAATGCTAT-3'; *crip2*\_forw: 5'-ATGGCTCCAAGT-GCCCAAGTGT-3'; *crip2*\_rev: 5'-CCATAGCAAGCCTTGTTGGCAGTAG-3'; *crip3*\_forw: 5'-CTTCGCAGAGAAAGTGAGCTCCTT-3'; *crip3*\_rev: 5'-CCG-TAGCATGGAAACATGGCAG-3'. The proof reading *PfuUltra*<sup>TM</sup> II fusion HS DNA polymerase (Agilent Tech., Santa Clara, CA) was used for all PCR reactions. Amplification accuracies and inserts orientation were confirmed by sequencing. Sequences were deposited at NCBI with the accession numbers KP036486 (*crip1*), KP036487 (*crip2*) and KP036488 (*crip3*).

### Protein alignment and synteny analyses, phylogenetic tree

The ClustalW2 program from the EMBL-EBI homepage was used for amino acid sequence alignment, homology calculation and generation of the phylogenetic tree. Following sequences were used: human CRIP1: NP\_001302.1, mouse Crip1 NP\_031789.1, rat Crip1: NP\_001231796.1, *X. tropicalis* Crip1: NP\_001165119.1, *X. laevis* Crip1-a: NP\_001087303.1, zebrafish Crip1: NP\_001153291.1, human CRIP2: NP\_001303.1, mouse Crip2: NP\_077185.1, rat Crip2: NP\_071946.1, *X. tropicalis* Crip2: NP\_001072735.1, zebrafish Crip2: NP\_998662.2, human CRIP3: NP\_996805.2, mouse Crip3 isoform TLP-A: NP\_858050.1 (homology) and isoform TLP-B: NP\_444480.1 (phylogenesis), rat Crip3: NP\_001102773.1, *X. tropicalis* Crip3: NP\_001015811.1. NCBI GeneBank and Xenbase Genome Browser v7.1 were used for synteny analyses, genomic structure and chromosomal organisation. Human, mouse, rat, *X. tropicalis* and zebrafish *crip1*, *crip2* and *crip3* were compared.

### RNA isolation and RT-PCR assays

To examine the temporal expression pattern of *crip1-3*, total RNA of *Xenopus* embryos at different developmental stages (stages 1 to 41) was isolated using the peq-GOLD RNAPure kit (Peqlab, Erlangen, D). cDNA was generated using random primers and the SuperScript II reverse transcriptase (Invitrogen, Carlsbad, CA). RT-PCRs were performed using the Phire Hot Start II DNA polymerase (Thermo Scientific, Waltham, MA) and following primers: GAPDH\_RT\_forw: 5'-GCCGTGTATGTGGTGGAAATCT-3'; GAPDH\_RT\_rev: 5'-AAGTTGTCGTGTGATGACCTTTGC-3'; *Crip1*\_RT\_forw: 5'-GGTATCCTCCCTGGGAAAAG-3'; *Crip1*\_RT\_rev: 5'-ATTGTCCT-

TABLE 1

### SPATIAL EXPRESSION OF ALL THREE CRIP FAMILY MEMBERS DURING XENOPUS LAEVIS EMBRYOGENESIS

	Brain		Retina	Cranial nerves	Branchial arches	Neural tube	Cardiovasc. system	Pronephros
	mb	hb						
<i>crip1</i>			+	+	+	+		+
<i>crip2</i>	+	+	+		+	+	+	+
<i>crip3</i>			+	+	+		+	+

hb hindbrain; md midbrain.

TACTCGGCACAC-3'; Crip2\_RT\_for: 5'-GCCCCAAGTGTGACAAGACT-3'; Crip2\_RT\_rev: 5'-GCTGGAAGCTTTGCTGAGAC-3'; Crip3\_RT\_for: 5'-CTTCGCAGAGAAAGTGAGCTCCTT-3'; Crip3\_RT\_rev: 5'-CCGTAGCATGGAACATGGCAG-3'. Note that *crip1* primers were designed using the previously published *Xenopus laevis* sequence (Acc. No. NM\_001093834.1) and therefore do not completely match with the sequence shown in Suppl. Fig. 1. Annealing temperatures were: gapdh: 55°C; crip1: 52°C; crip2: 51°C; crip3: 54°C and the product lengths were: gapdh: 230 bp; crip1: 366 bp; crip2: 332bp; crip3: 488 bp.

#### Dot blot

Dot blotting using Hybond-N<sup>+</sup> nucleic acid transfer membranes (GE Healthcare, Cleveland, Ohio) was done to test RNA probes for their specificity. 1 µg of plasmid DNA of *crip1-3* was diluted in 2x SSC buffer, denatured, dot blotted and hybridized with *crip1-3* digoxigenin-labeled antisense RNA probes according to the manufacturer's instruction (GE Healthcare, 9.5 protocol for dot blotting and 10.2 hybridization protocol). Blocking and staining of the blots with BM-Purple (Roche, Basel) was done according to the WMISH protocol.

#### Whole mount in situ hybridization (WMISH) and sectioning

To investigate the spatio-temporal expression of *crip1-3* digoxigenin-labeled antisense RNA probes were generated by *in vitro* transcription with either T7 or T3 RNA polymerase (Roche, Basel). WMISH analyses were performed according to established protocols (Hemmati-Brivanlou *et al.*, 1990) using fixed *Xenopus* embryos at different developmental stages, which were subsequently stained with BM-Purple (Roche, Basel). For more detailed analyses of the gene expressions vibratome sections of 25 µm thickness were performed as previously described (Guo *et al.*, 2011).

#### Acknowledgements

Annemarie Hempel is a member of the International Graduate School in Molecular Medicine of Ulm University (GSC270). We thank especially Karin Botzenhart and Petra Dietmann for their technical support.

#### References

- BACH, I. (2000). The LIM domain: regulation by association. *Mech Dev* 91: 5-17.
- BIRKENMEIER, E.H. and GORDON, J.I. (1986). Developmental regulation of a gene that encodes a cysteine-rich intestinal protein and maps near the murine immunoglobulin heavy chain locus. *Proc Natl Acad Sci USA* 83: 2516-2520.
- CASROUGE, A., VEITIA, R., KIRCHNER, J., BEVAN, M.J. and KANELLOPOULOS, J. (2004). The human and mouse orthologous LIM-only proteins respectively encoded in chromosome 6 and 17 show a different expression pattern. *Microbes Infect* 6: 1063-1072.
- CHUNG, Y.C., TSAI, Y.J., SHIU, T.Y., SUN, Y.Y., WANG, P.F. and CHEN, C.L. (2011). Screening large numbers of expression patterns of transcription factors in late stages of the mouse thymus. *Gene Expr Patterns* 11: 84-92.
- DAVIS, B.A., BLANCHARD, R.K., LANNINGHAM-FOSTER, L. and COUSINS, R.J. (1998). Structural characterization of the rat cysteine-rich intestinal protein gene and overexpression of this LIM-only protein in transgenic mice. *DNA Cell Biol* 17: 1057-1064.
- GUO, Y., CHRISTINE, K.S., CONLON, F., GESSERT, S. and KUHL, M. (2011). Expression analysis of *epb4114a* during *Xenopus laevis* embryogenesis. *Dev Genes Evol* 221: 113-119.
- HALLQUIST, N.A., KHOO, C. and COUSINS, R.J. (1996). Lipopolysaccharide regulates cysteine-rich intestinal protein, a zinc-finger protein, in immune cells and plasma. *J Leukoc Biol* 59: 172-177.
- HEMMATI-BRIVANLOU, A., FRANK, D., BOLCE, M.E., BROWN, B.D., SIVE, H.L. and HARLAND, R.M. (1990). Localization of specific mRNAs in *Xenopus* embryos by whole-mount *in situ* hybridization. *Development* 110: 325-330.
- HEMPE, J.M. and COUSINS, R.J. (1991). Cysteine-rich intestinal protein binds zinc during transmucosal zinc transport. *Proc Natl Acad Sci USA* 88: 9671-9674.
- HEMPE, J.M. and COUSINS, R.J. (1992). Cysteine-rich intestinal protein and intestinal metallothionein: an inverse relationship as a conceptual model for zinc absorption in rats. *J Nutr* 122: 89-95.
- KARIM, M.A., OHTA, K., EGASHIRA, M., JINNO, Y., NIIKAWA, N., MATSUDA, I. and INDO, Y. (1996). Human ESP1/CRP2, a member of the LIM domain protein family: characterization of the cDNA and assignment of the gene locus to chromosome 14q32.3. *Genomics* 31: 167-176.
- KHOO, C., HALLQUIST, N.A., SAMUELSON, D.A. and COUSINS, R.J. (1996). Differential expression of cysteine-rich intestinal protein in liver and intestine in CCl4-induced inflammation. *Am J Physiol* 270: G613-G618.
- KIRCHNER, J., FORBUSH, K.A. and BEVAN, M.J. (2001). Identification and characterization of thymus LIM protein: targeted disruption reduces thymus cellularity. *Mol Cell Biol* 21: 8592-8604.
- LANNINGHAM-FOSTER, L., GREEN, C.L., LANGKAMP-HENKEN, B., DAVIS, B.A., NGUYEN, K.T., BENDER, B.S. and COUSINS, R.J. (2002). Overexpression of CRIP in transgenic mice alters cytokine patterns and the immune response. *Am J Physiol Endocrinol Metab* 282: E1197-E1203.
- LEVENSON, C.W., SHAY, N.F., LEE-AMBROSE, L.M. and COUSINS, R.J. (1993). Regulation of cysteine-rich intestinal protein by dexamethasone in the neonatal rat. *Proc Natl Acad Sci USA* 90: 712-715.
- LIEBHABER, S.A., EMERY, J.G., URBANEK, M., WANG, X.K. and COOKE, N.E. (1990). Characterization of a human cDNA encoding a widely expressed and highly conserved cysteine-rich protein with an unusual zinc-finger motif. *Nucleic Acids Res* 18: 3871-3879.
- NALIK, P., PANAYOTOVA-HEIERMANN, M. and PONGS, O. (1989). Characterization of an estradiol-stimulated mRNA in the brain of adult male rats. *Mol Cell Endocrinol* 62: 235-242.
- NIEUWKOOP, P.D. and FABER, J. (1994). *Normal table of Xenopus laevis (Daudin): a systematical and chronological survey of the development from the fertilized egg till the end of metamorphosis*. Garland Pub., New York.
- OKANO, I., YAMAMOTO, T., KAJI, A., KIMURA, T., MIZUNO, K. and NAKAMURA, T. (1993). Cloning of CRP2, a novel member of the cysteine-rich protein family with two repeats of an unusual LIM/double zinc-finger motif. *FEBS Lett* 333: 51-55.
- SIVE, H.L., GRAINGER, R.M. and HARLAND, R.M. (2000). *Early development of Xenopus laevis: a laboratory manual*. Cold Spring Harbor Laboratory Press, Cold Spring Harbor, N.Y.
- SUN, X., ZHANG, R., LIN, X. and XU, X. (2008). Wnt3a regulates the development of cardiac neural crest cells by modulating expression of cysteine-rich intestinal protein 2 in rhombomere 6. *Circ Res* 102: 831-839.
- TANABE, C., HOTODA, N., SASAGAWA, N., FUTAI, E., KOMANO, H. and ISHIURA, S. (2010). ADAM19 autolysis is activated by LPS and promotes non-classical secretion of cysteine-rich protein 2. *Biochem Biophys Res Commun* 396: 927-932.
- TSUI, S.K., YAM, N.Y., LEE, C.Y. and WAYE, M.M. (1994). Isolation and characterization of a cDNA that codes for a LIM-containing protein which is developmentally regulated in heart. *Biochem Biophys Res Commun* 205: 497-505.
- VAN HAM, M., CROES, H., SCHEPENS, J., FRANSEN, J., WIERINGA, B. and HENDRIKS, W. (2003). Cloning and characterization of mCRIP2, a mouse LIM-only protein that interacts with PDZ domain IV of PTP-BL. *Genes Cells* 8: 631-644.
- WANG, W., ZHANG, L.F., GUI, Y.H. and SONG, H.Y. (2013). Retinol dehydrogenase, RDH11, is essential for the heart development and cardiac performance in zebrafish. *Chin Med J (Engl)* 126: 722-728.
- WANG, X., LEE, G., LIEBHABER, S.A. and COOKE, N.E. (1992). Human cysteine-rich protein. A member of the LIM/double-finger family displaying coordinate serum induction with c-myc. *J Biol Chem* 267: 9176-9184.
- WEI, T.C., LIN, H.Y., LU, C.C., CHEN, C.M. and YOU, L.R. (2011). Expression of Crip2, a LIM-domain-only protein, in the mouse cardiovascular system under physiological and pathological conditions. *Gene Expr Patterns* 11: 384-394.
- WIESE, C.B., IRELAND, S., FLEMING, N.L., YU, J., VALERIUS, M.T., GEORGAS, K., CHIU, H.S., BRENNAN, J., ARMSTRONG, J., LITTLE, M.H. *et al.*, (2012). A genome-wide screen to identify transcription factors expressed in pelvic ganglia of the lower urinary tract. *Front Neurosci* 6: 130.
- YU, T.S., MOCTEZUMA-ANAYA, M., KUBO, A., KELLER, G. and ROBERTSON, S. (2002). The heart LIM protein gene (Hlp), expressed in the developing and adult heart, defines a new tissue-specific LIM-only protein family. *Mech Dev* 116: 187-192.
- ZHANG, L., HOFFMAN, J.A. and RUOSLAHTI, E. (2005). Molecular profiling of heart endothelial cells. *Circulation* 112: 1601-1611.

**Further Related Reading, published previously in the *Int. J. Dev. Biol.***

**Sexual dimorphism of AMH, DMRT1 and RSPO1 localization in the developing gonads of six anuran species**

Rafal P. Piprek, Anna Pecio, Katarzyna Laskowska-Kaszub, Jacek Z. Kubiak and Jacek M. Szymura  
Int. J. Dev. Biol. (2013) 57: 891-895

**Dual embryonic origin of the hyobranchial apparatus in the Mexican axolotl (*Ambystoma mexicanum*)**

Asya Davidian and Yegor Malashichev  
Int. J. Dev. Biol. (2013) 57: 821-828

**Clonal analyses in the anterior pre-placodal region: implications for the early lineage bias of placodal progenitors**

Sujata Bhattacharyya and Marianne E. Bronner  
Int. J. Dev. Biol. (2013) 57: 753-757

**Amphibian interorder nuclear transfer embryos reveal conserved embryonic gene transcription, but deficient DNA replication or chromosome segregation**

Patrick Narbonne and John B. Gurdon  
Int. J. Dev. Biol. (2012) 56: 975-986

**Origins of Cdx1 regulatory elements suggest roles in vertebrate evolution**

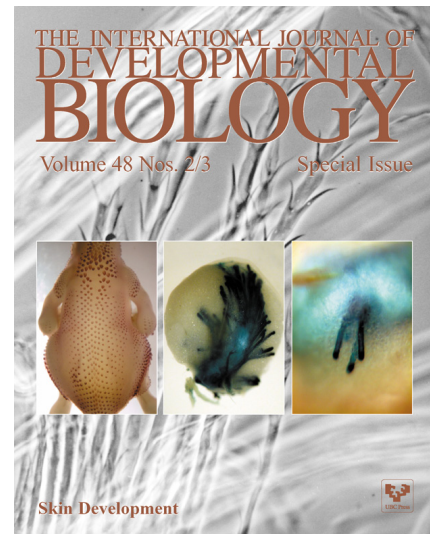
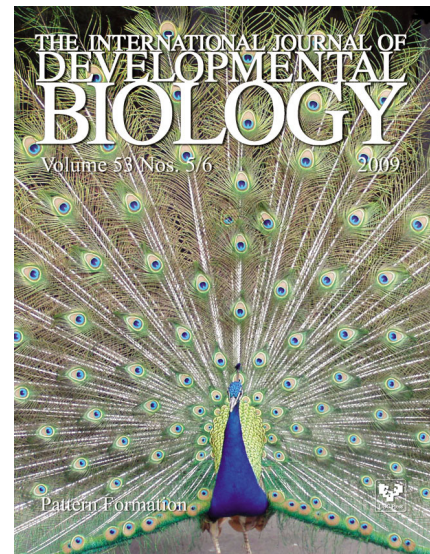
Stephen J. Gaunt and Yu-Lee Paul  
Int. J. Dev. Biol. (2011) 55: 93-98

**Reptile scale paradigm: Evo-Devo, pattern formation and regeneration**

Cheng Chang, Ping Wu, Ruth E. Baker, Philip K. Maini, Lorenzo Alibardi and Cheng-Ming Chuong  
Int. J. Dev. Biol. (2009) 53: 813-826

**Proteomics analysis of regenerating amphibian limbs: changes during the onset of regeneration**

Michael W. King, Anton W. Neff and Anthony L. Mescher  
Int. J. Dev. Biol. (2009) 53: 955-969



**5 yr ISI Impact Factor (2013) = 2.879**

